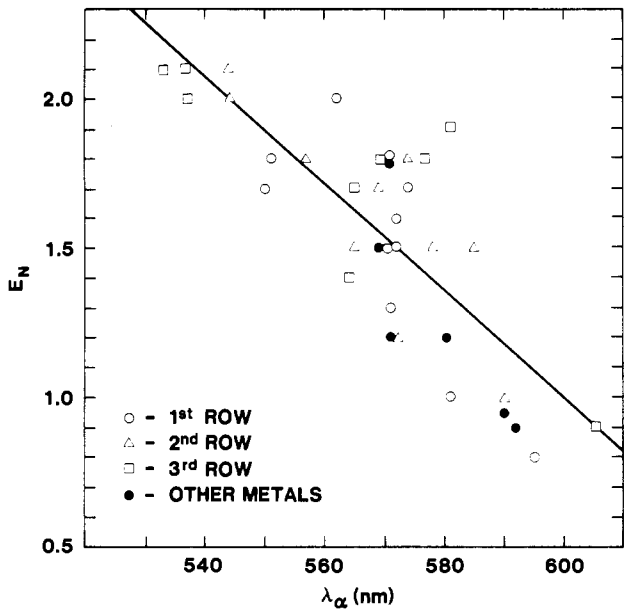

Figure 2. Correlation between electronegativity and λ_α for metalloporphyrins with normal and hypso absorption spectra. See Table I. The correlation coefficient is 0.80. Electronegativities of Zhang[52,53] and Sanderson[54,55] gave correlation coefficients between 0.76 and 0.83. Zhang gives electronegativities for different oxidation states of metals obtained from ionization potentials. Either (1) an ionic bonding term must be added, (2) +4 and +5 oxidation states must be omitted, or (3) +2 oxidation-state values must be used. Otherwise, the correlation coefficient is only 0.59, and the high-oxidation-state metalloporphyrins show a systematic error.

al-bonding atoms in metalloporphyrins and the range of E_N for the metals is 0.8–2.2 (see Table I), any increase in metal electronegativity would result in a smaller difference in E_N values and, therefore, increase covalency of the metal–porphyrin bond. The immediate consequences of increased E_N upon the electronic distribution within the porphyrin ring would be increased σ donation to the metal and enhanced π back-donation to the ring.

The relationship between λ_α and E_N in Figure 2 therefore suggests that λ_α is a direct measure of the covalency of the metal–porphyrin bond. Moreover, the degree of covalency might be expected to influence porphyrin geometry in a predictable manner. An indication of this is found in the monotonic dependence of calculated values of σ- and π-ring charge densities, which reflect the degree of covalency for a group of first-row metals and the frequencies of the Raman core-size-sensitive modes.[9]

The correlations in Figure 1 between porphyrin core size and covalency as measured by λ_α can now be explained as follows: (a) Within a row, the more electronegative metals form a tighter, more covalent bond resulting in a smaller core size and, therefore, higher ν_{10} frequency. (b) In the next row down, the valence orbitals have larger spatial extent, and, hence, a larger core size gives the same degree of interaction with the metal orbitals and covalency of the metal–porphyrin bond. This accounts for the shift along the λ_α axis toward higher covalency (lower λ_α) for equal core size when comparing upper row metals with lower row metals.

The correlations presented suggest a direct relationship between porphyrin geometry (as modulated by covalency of the metal–porphyrin bond) and the energetics of the porphyrin π system, indicating that, over the range of metals investigated, the degree of metal–porphyrin covalency affects the $a_{2u}(\pi)$ and $e_g(\pi^*)$ orbital energies in a concerted fashion.[9,29] It should be noted however that a unique relationship between porphyrin electronic transitions and geometry does not exist. For metal substitution and in some cases of axial ligation (e.g., for VO and $V(OH)_2$ porphyrins (see Figure 1) and for Cu porphyrins[51]) λ_α is *inversely proportional* to ν_{10}. In contrast, λ_α is *proportional* to ν_{10} for other cases of axial ligation[28] and for formation of complexes with π acceptors.[28-30,41] Therefore, the response of both λ_α and ν_{10} to changes in a metalloporphyrin's interaction with its surroundings carries more information than the shift in either of these spectroscopic parameters alone.

Acknowledgment. We thank Martin Gouterman for helpful discussions concerning his calculations.

(51) Shelnutt, J. A.; Straub, K. D.; Rentzepis, P. M.; Gouterman, M.; Davidson, E. R. *Biochemistry*, in press.
(52) Zhang, Y. *Inorg. Chem.* **1982**, *21*, 3886.
(53) Zhang, Y. *Inorg. Chem.* **1982**, *21*, 3889.
(54) Sanderson, R. T. *J. Am. Chem. Soc.* **1983**, *105*, 2259.
(55) Sanderson, R. T. "Polar Covalence"; Academic Press: New York, 1983.

Contribution from the Department of Chemistry, University of California, Riverside, California 92521

Resonance Raman Spectra of the Carbon-Bridged Iron Porphyrin Dimer (μ-Carbido)bis[(5,10,15,20-tetraphenylporphinato)iron]

Joseph A. Hofmann, Jr., and David F. Bocian*[1]

Received July 8, 1983

The characterization of model (porphinato)iron complexes containing metal ions with valence states greater than Fe(III) is of current interest,[2-6] in large part because highly oxidized porphyrin complexes serve as intermediates in a number of heme protein reactions.[7-9] One type of model complex that has attracted attention[2,3,10] is the series of neutral and oxidized single-atom bridged dimers of the form $((TPP)Fe)_2X$ (TPP = tetraphenylporphyrin; X = O, N,[11,12] C[13]). The Fe ions of $((TPP)Fe)_2O$ are known to be high-spin Fe(III).[14] On the other hand $((TPP)Fe)_2N$ and $((TPP)Fe)_2C$ contain low-spin Fe ions.[13,15] Recent Mössbauer studies[10] indicate that the

(1) Alfred P. Sloan Foundation Fellow, 1982–1984.
(2) Felton, R. H.; Owen, G. S.; Dolphin, D.; Fajer, J. *J. Am. Chem. Soc.* **1971**, *93*, 6332.
(3) Shimomura, E. T.; Phillipi, M. A.; Goff, H. M.; Scholtz, W. F.; Reed, C. A. *J. Am. Chem. Soc.* **1981**, *103*, 6778.
(4) Phillipi, M. A.; Goff, H. M. *J. Am. Chem. Soc.* **1982**, *104*, 6026.
(5) Gans, P.; Marchon, J. C.; Reed, C. A.; Regnard, J. R. *Nouv. J. Chim.* **1981**, *5*, 201.
(6) Simonneaux, G.; Sholtz, W. F.; Reed, C. A.; Lang, G. *Biochim. Biophys. Acta* **1982**, *716*, 1.
(7) Reid, T. V.; Murthy, M. R. N.; Sicignanu, A.; Tanaka, N.; Musick, W. D. L.; Rossman, M. G. *Proc. Natl. Acad. Sci. U.S.A.* **1981**, *78*, 4767.
(8) Hewson, W. D.; Hager, L. P. In "The Porphyrins"; Dolphin, D., Ed.; Academic Press: New York, 1979; Vol. 7, pp 295–332.
(9) Griffin, B. W.; Peterson, J. A.; Eastbook, R. W. In "The Porphyrins"; Dolphin, D., Ed.; Academic Press: New York, 1979; Vol. 4, pp 197–256.
(10) English, D. R.; Hendrickson, D. N.; Suslick, K. S. *Inorg. Chem.* **1983**, *22*, 367.
(11) Summerville, D. A.; Cohen, I. A. *J. Am. Chem. Soc.* **1976**, *98*, 1747.
(12) Kadish, K. M.; Rhodes, R. K.; Bottomley, L. A.; Goff, H. M. *Inorg. Chem.* **1981**, *20*, 3195.
(13) Mansuy, D.; Lecomte, J. P.; Chottard, J. C.; Bartoli, J. F. *Inorg. Chem.* **1981**, *20*, 3119.
(14) Murray, K. S. *Coord. Chem. Rev.* **1974**, *12*, 1.
(15) Kadish, K. M.; Bottomley, L. A.; Brace, J. G.; Winograd, N. *J. Am. Chem. Soc.* **1980**, *102*, 4341.

0020-1669/84/1323-1177$01.50/0

electron density on the metal ions in the nitrogen-bridged dimer is less than in the oxygen-bridged complex and that the density in the carbon-bridged dimer is less than both of the other systems. This leads to a formulation of the bridging systems in the nitrogen and carbon dimers as Fe($III^1/_2$)–nitride–Fe($III^1/_2$) and Fe(IV)–carbide–Fe(IV).

Resonance Raman (RR) spectroscopy provides a sensitive probe of the structure and properties of (porphinato) iron compexes.[16,17] Detailed RR studies have been reported for ((TPP)Fe)$_2$O[18] and ((TPP)Fe)$_2$N,[19] but only limited RR data are available for ((TPP)Fe)$_2$C.[20] The Raman frequencies observed for the three ((TPP)Fe)$_2$X complexes clearly reflect the high-spin character of the metal ions for X = O[18] and the low-spin character for X = N[19b] and C.[20] The electron densities on the metal centers of ((TPP)Fe)$_2$N and ((TPP)Fe)$_2$C relative to ((TPP)Fe)$_2$O cannot be readily ascertained from the RR data, since the bands sensitive to this property are also sensitive to the spin state of the metal ions.[20,21] However, the metal ion spin densities of the two low-spin complexes can be compared with one another via their RR frequencies.

We report here the results of a detailed RR study on ((TPP)Fe)$_2$C using a large number of excitation wavelengths throughout the Soret and visible regions. These studies result in a better characterization of the carbon-bridged dimer.

Experimental Section

The ((TPP)Fe)$_2$C complex was prepared and purified as described in ref 13. Substitution of ^{54}Fe (from $^{54}Fe_2O_3$, 97.08% in ^{54}Fe, Oak Ridge National Laboratories) was accomplished in a manner similar to that outlined in ref 18a. The formation of the complexes was monitored by using UV–vis spectroscopy and confirmed by the appearance of the asymmetric Fe–C–Fe stretching mode in the IR spectrum. All solvents were spectral grade and used without further purification.

The RR spectra were recorded with the optics in a 90° scattering configuration using an apparatus described previously.[19b] RR spectra were obtained for both solid samples (in 1:1 NaCl/Na_2WO_4 pellets) and CS_2 solutions. Sample concentrations in the pellets were 1.5 mg/250 mg of host. Concentrations in solutions were 0.2 mg/mL for B-state excitation and 1.0 mg/mL for Q-state excitation. All solution samples were cooled (273 K), deoxygenated, and flowed to prevent photodecomposition. Sample integrity was monitored by using the RR spectrum and UV–vis spectroscopy. B-state-excitation RR spectra were collected at 2-cm^{-1} intervals at rates of 5–12 s/point with a spectral slit width of 3 cm^{-1}. The incident laser power was less than 10 mW. Isotope shifts were measured from spectra recorded at comparable count rates with similar laser powers but with count intervals of 0.2 cm^{-1} and a spectral slit width of 0.5 cm^{-1}. Q-state-excitation RR spectra were collected at 2-cm^{-1} intervals at rates of 4–20 s/point with a spectral slit width of 4 cm^{-1}. The incident laser powers ranged from 15–50 mW. Excitation profiles were obtained for solid samples (in 1:1 NaCl/Na_2WO_4 pellets). The 934-cm^{-1} Na_2WO_4 band was as an intensity standard. The other spectral conditions were the same as those given above for Q-state excitation. The profiles were corrected for the ν^4 dependence of scattered light and instrument and photomultiplier responses.

Results and Discussion

The RR spectra of solid ((TPP)Fe)$_2$C in 1:1 NaCl/Na_2WO_4 pellets observed with excitation near the maxima of the Soret (λ_{ex} 4067 Å) and visible (λ_{ex} 5309 Å) bands are shown in Figure 1. The RR spectra obtained in CS_2 solution are identical with those of the solid except that a few of the bands show slight shifts (~2 cm^{-1}) in frequency. The frequencies of the observed RR bands are listed in Table I and categorized according to D_{4h} symmetry classiciations as determined by their depolarization ratios, ρ: A_{1g}, $\rho < 0.75$ (polarized); A_{2g}, $\rho > 0.75$ (anomalously polarized); B_{1g} and B_{2g}, $\rho = 0.75$ (depolarized). The spectrum observed with λ_{ex} 4067 Å exhibits only polarized bands, indicative of the Franck–Condon scattering mechanisms typically in effect upon excitation of the

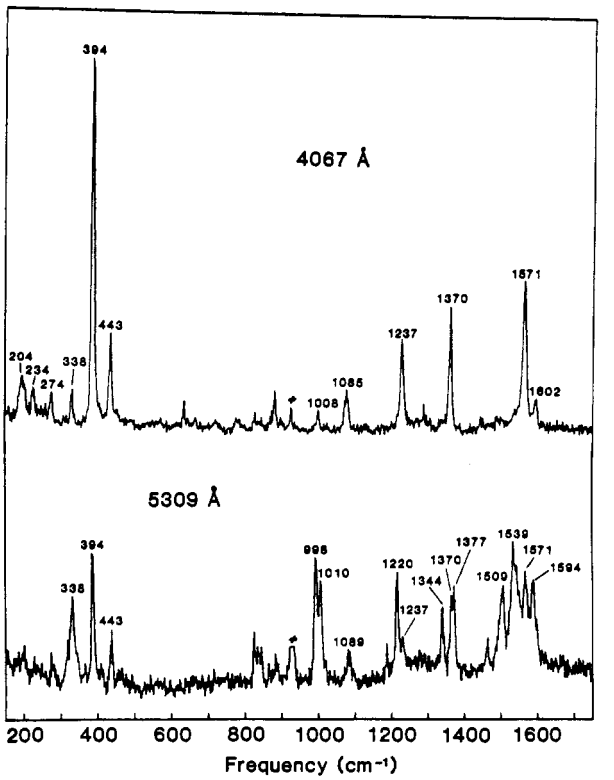

Figure 1. Resonance Raman spectra of solid ((TPP)Fe)$_2$C in a 1:1 NaCl/Na_2WO_4 pellet. Peaks due to Na_2WO_4 are denoted by #. See the Experimental Section for spectral conditions.

Table I. Comparison of the Principal RR Bands (cm^{-1}) of ((TPP)Fe)$_2$C, ((TPP)Fe)$_2$N, and ((TPP)Fe)$_2$O

sym	band	((TPP)-Fe)$_2$C[a]	((TPP)-Fe)$_2$N[b]	((TPP)-Fe)$_2$O[c]	assgnt[d]
A_{1g}	1	1602	1599	1599	phenyl
	2	1571	1567	1553	$\nu(C_\beta C_\beta) + \delta(C_\beta H)$
	3	1370	1367	1359	$\nu(C_\alpha N) + \delta(C_\beta H)$
	4	1237	1235	1237	$\nu(C_m\text{-Ph})$
	5	1085	1080	1083	$\delta(C_\beta H)$
	6	1008	1004	1004	$\nu(C_\alpha C_m)$
	7	998	996	995	phenyl
	8	443	424	363	ν_s(Fe-X-Fe)
	9	394	386	390	porphyrin def
	10	338	336	330	out-of-plane def
	11	274	267		
	12	234	226		
	13	204	194		
A_{2g}	14	1539	1538	1511	$\nu(C_\alpha C_m)$
	15	1344	1342	1333	$\nu(C_\alpha C_\beta) + \delta(C_\beta H)$
	16	1220	1226	1234	$\nu(C_\alpha N) + \delta(C_\beta H)$
B_{1g} and B_{2g}	17	1594	1588	1561	$\nu(C_\alpha C_m)$
	18	1509	1506	1495	$\nu(C_\beta C_\beta)$
	19	1377	1374	1368	
	20	1089	1088	1087	$\delta(C_\beta H)$
	21	1010	1012	1014	$\delta(C_\beta H)$

[a] This work. [b] Reference 19b. [c] Reference 18a. [d] The subscripts in the assignment labels identify the pyrrole α and β and the bridging-methine carbon atoms in the porphyrin macrocycle. Ph refers to the phenyl groups.

(16) Spiro, T. G. In "Iron Porphyrins"; Lever, A. B. P., Gray, H. B., Eds.; Addison-Wesley: Reading, MA, 1982; Part II, pp 89–152.
(17) Felton, R. H.; Yu, N.-T. In "The Porphyrins"; Dolphin, D., Ed.; Academic Press: New York, 1978; Vol. 2, pp 347–388.
(18) (a) Burke, J. M.; Kincaid, J. R.; Spiro, T. G. *J. Am Chem. Soc.* **1978**, *100*, 6077. (b) Adar, F.; Srivastava, T. S. *Proc. Natl. Acad. Sci. U.S.A.* **1975**, *72*, 4419.
(19) (a) Schick, G. A.; Bocian, D. F. *J. Am. Chem. Soc.* **1980**, *102*, 7982; (b) *Ibid* **1983**, *105*, 1830.
(20) Chottard, G.; Battioni, P. Battioni, J.-P.; Lang, M.; Mansuy, D. *Inorg. Chem.* **1981**, *20*, 1718.
(21) Burke, J. M.; Kincaid, J. R.; Peters, S.; Gagne, R. R.; Collman, J. P.; Spiro, T. G. *J. Am. Chem. Soc.* **1978**, *100*, 6083.

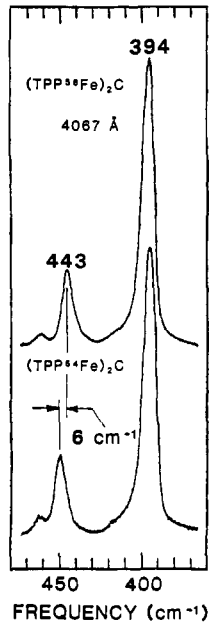

Figure 2. Low-frequency resonance Raman spectra of $((TPP)Fe)_2C$ in a 1:1 $NaCl/Na_2WO_4$ pellet showing the isotope shift of the 443-cm^{-1} band. See the Experimental Section for spectral conditions.

intense Soret band of metalloporphyins.[22] Conversely, the RR spectrum obtained with λ_{ex} 5309 Å exhibits mostly depolarized and anomalously polarized bands, indicative of the vibronic scattering mechanisms operative upon excitation of the less intense visible bands.[22-24] There are several polarized bands observed with visible region excitation, in part due to the substantial Soret intensity underlying the visible absorption. However, certain polarized bands, notably the 998-, 443-, 394-, and 338-cm^{-1} bands, do display intrinsic Q-state scattering.

Virtually all of the RR bands of $((TPP)Fe)_2C$ observed with Soret and visible region excitation are in-plane porphyrin modes and have analogues in the RR spectra of $((TPP)Fe)_2N$[19b] and $((TPP)Fe)_2O$.[18a] We have assigned these bands of the carbon-bridged complex by comparison with those of the other two dimers. The RR frequencies for $((TPP)Fe)_2N$ and $((TPP)Fe)_2O$ are also listed in Table I along with the assignments for the normal-mode compositions.

Other prominent RR bands are observed for $((TPP)Fe)_2C$, which are not due to in-plane porphyrin skeletal modes. However, most of these bands can also be assigned by analogy to $((TPP)Fe)_2N$ and $((TPP)Fe)_2O$ (Table I). High-frequency bands are observed at 1602 and 998 cm^{-1} due to enhanced internal vibrations of the C_m phenyl groups. The intensity of the 998-cm^{-1} band is quite large with λ_{ex} 5309 Å, similar to that observed for this mode in $((TPP)Fe)_2N$. A set of four low-frequency bands is observed in the region 200–350 cm^{-1}, which have analogues in the RR spectra of $((TPP)Fe)_2N$. These bands are due to out-of-plane deformations of the porphyrin skeleton.[19b] The intense band at 443 cm^{-1} is also an out-of-plane mode. Its assignment as the symmetric Fe–C–Fe stretching vibration will be discussed further below.

Most of the RR features we observe for $((TPP)Fe)_2C$ are in reasonable agreement with those reported previously;[20] however, there are several significant differences. First, we observe the oxidation state sensitive band 3 at 1370 cm^{-1} rather than at 1365 cm^{-1}. (It should be noted that band 3 is observed at 1368 cm^{-1} in CS_2 solutions.) Second, an intense band is seen at 443 cm^{-1} with both visible and Soret excitation, which

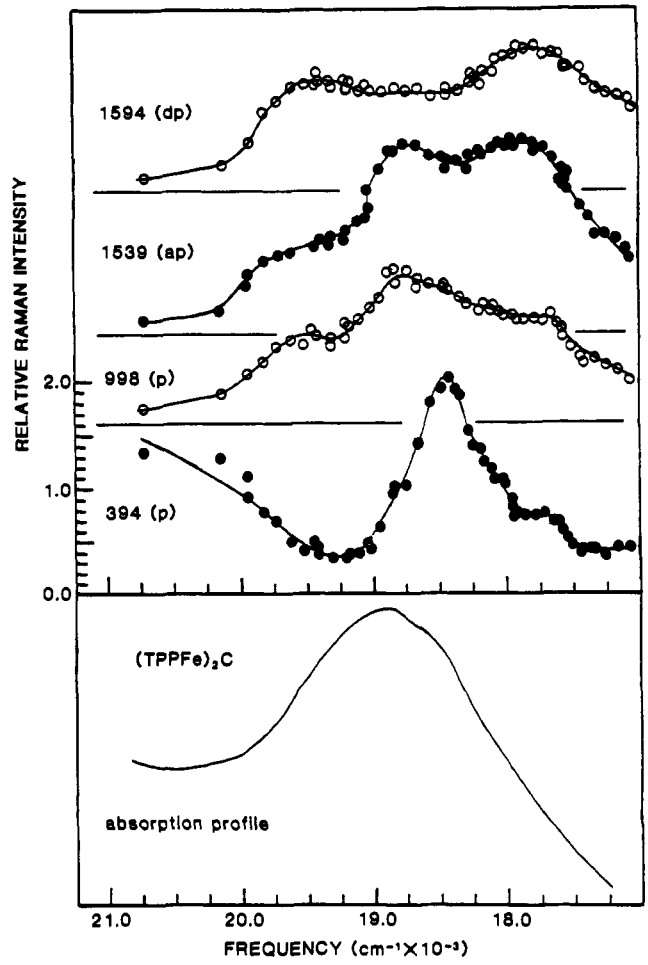

Figure 3. Visible-region-excitation profiles for representative bands of solid $((TPP)Fe)_2C$ in 1:1 $NaCl/Na_2WO_4$ pellets. The intensities are plotted on a linear scale of magnitude 10^2 relative to the 934-cm^{-1} band of Na_2WO_4. The profiles are displaced vertically and are plotted by using alternately filled (●) and open (○) circles for clarity of presentation. The visible-region-absorption profile is also shown. Abbreviations: p, polarized; dp, depolarized, ap, anomalously polarized.

was not observed previously. Finally, we do not observe a band at 1555 cm^{-1} as was previously reported. We have found that none of these spectral differences can be attributed to solvent or medium effects. Instead, the variance observed in the three spectral features between the present and previous RR study of $((TPP)Fe)_2C$ is due to photodecomposition of the sample in the latter case. The $((TPP)Fe)_2C$ complex is particularly photosensitive in solutions that have not been rigorously deoxygenated. Less than 1 min of either Soret or visible wavelength irradiation of oxygen-containing solutions of the dimer with laser powers of ~10 mW is sufficient to photolyze a substantial amount of the sample. The photolysis can be monitored by observing the spectral changes noted above. Similar photolysis problems have been noted for $((TPP)Fe)_2N$.[19b] Solid samples of this material as well as of $((TPP)Fe)_2C$ show much improved photostability.

The location of the oxidation state sensitive band 3 of $((TPP)Fe)_2C$ and $((TPP)Fe)_2N$ at nearly the same frequency is significant, given the relatively small frequency range exhibited by this band in low-spin FeTPP complexes (typically 10 cm^{-1} or less between Fe(II) and Fe(III)[20,21]). The increased π-donor capability of X = C compared to that of X = N[25] should tend to lower the frequency of band 3 in the former complex relative to the latter.[16] The fact that the frequency is similar for the two complexes suggests that the electron density on the Fe ions

(22) Clark, R. J. H.; Stewart, B. *Struct. Bonding (Berlin)* **1979**, *36*, 1.
(23) Shelnutt, J. A.; Cheung, L. D.; Chang, R. C. C.; Yu, N.-T.; Felton, R. H. *J. Am. Chem. Phys.* **1977**, *66*, 3387.
(24) Shelnutt, J. A.; O'Shea, D. C. *J. Chem. Phys.* **1978**, *69*, 5361.
(25) Tatsumi, K.; Hoffmann, R. *J. Am. Chem. Soc.* **1981**, *103*, 3328.

in the carbon-bridged dimer is lower than in the nitrogen-bridged complex, counterbalancing the π-donor effect. This is consistent with the recent Mössbauer studies of the two complexes.[10]

The low-frequency and photosensitivity of the 443-cm^{-1} band suggests that this mode is an out-of-plane deformation associated with the Fe–C–Fe linkage. In this regard, the symmetric Fe–X–Fe stretching vibrations of $((TPP)Fe)_2O$[18a] and $((TPP)Fe)_2N$[19b] are observed in the RR spectra at 363 and 424 cm^{-1}, respectively. We have assigned the 443-cm^{-1} band of $((TPP)Fe)_2C$ as the analogous mode on the basis of its ^{54}Fe isotope shift. RR spectra of $((TPP)^{56}Fe)_2C$ and $((TPP)^{54}Fe)_2C$ in the frequency range 360–480 cm^{-1} are compared in Figure 2. The substitution of ^{54}Fe results in a shift of the 443-cm^{-1} band 6 cm^{-1} to higher frequency. Only very small shifts (1–2 cm^{-1}) are observed for the other out-of-plane modes. The 6-cm^{-1} upshift represents 75% of the theoretical value expected on the basis of the change in reduced mass for the motion.

The frequencies of the symmetric (443-cm^{-1}) and asymmetric (939-cm^{-1}) Fe–C–Fe stretches can be used to calculate the valence force constants for the vibrations. The observed frequencies correspond to an Fe–C stretching constant of 4.6 mdyn/Å with a stretch–stretch interaction constant of 1.8 mdyn/Å. The Fe–C stretching force constant is larger than the Fe–N (4.5 mdyn/Å)[19b] and Fe–O (3.8 mdyn/Å)[18a] stretching constants, reflecting the higher bond order in the carbon bridge relative to that of the nitrogen and oxygen bridges.[25]

The visible region excitation profiles of several RR bands of solid $((TPP)Fe)_2C$ are shown in Figure 3 along with the absorption spectrum. The errors in the intensity measurements are on the order of ±10%, which results in errors in the peak positions in the profiles of ±150 cm^{-1}. The profiles indicate that the maximum in the absorption spectrum at 18 900 cm^{-1} (529 nm) corresponds to the Q(0,1) band and that the electronic origin Q(0,0) is located near 17 700 cm^{-1} (565 nm), although the latter band is not observed in the absorption spectrum.

The features of the excitation profiles of most of the RR bands of $((TPP)Fe)_2C$ are quite similar to those of the analogous bands of $((TPP)Fe)_2N$.[19b] As in the case for the nitrogen-bridged complex, the anomalously polarized modes in general show the strongest vibronic activity. This is evidenced by the multiple maxima[24] in the profile of the 1539-cm^{-1} band, which is representative of these modes. The strong vibronic coupling observed for the anomalously polarized modes can be contrasted with the much weaker coupling exhibited by the depolarized modes. The profile of the 1594-cm^{-1} band, which is representative of these latter vibrations, displays predominantly Q(0,0) and Q(0,1) maxima approximately separated by the ground-state vibrational frequency. Only a few polarized bands are observed with visible region excitation. The profiles for most of these bands cannot be measured accurately due to overlap with much stronger depolarized and anomalously polarized bands. The polarized bands with the largest RR activity in the visible region are the 998-cm^{-1} phenyl mode and the 394-cm^{-1} porphyrin deformation. The profile for each of these modes shows a peak at Q(0,0) and Q(0,1); however, a strong peak is also observed in the profile of each mode at roughly twice the ground-state vibrational frequency. These tertiary peaks could correspond to Q(0,2) maxima. The strong vibronic coupling apparently in effect for these two vibrations is undoubtedly responsible for their significantly greater Q-state RR activity relative to the other totally symmetric vibrations.

Acknowledgment is made to the donors of the Petroleum Research Fund, administered by the American Chemical Society, the Cottrell Research Grants Program of the Research Corp., the Committee on Research, University of California, Riverside, and the National Institute of General Medical Sciences (Grant GM-30078-01A1) for support of this research. Partial funding for the Raman spectrometer was provided by the Biomedical Research Support Grant Program of the U.S. Public Health Service.

Registry No. $((TPP)Fe)_2C$, 75249-87-5.